# Variation and Trend of Nitrate radical reactivity towards volatile organic compounds in Beijing, China

Hejun Hu[1], Haichao Wang[1, 2 *], Keding Lu[3*], Jie Wang[1], Zelong Zheng[1], Xuezhen Xu[1], Tianyu Zhai[3], Xiaorui Chen[4], Xiao Lu[1, 2], Wenxing Fu[5], Xin Li[3], Limin Zeng[3], Min Hu[3], Yuanhang Zhang[3], Shaojia Fan[1, 2]

[1]School of Atmospheric Sciences, Sun Yat-sen University, and Southern Marine Science and Engineering Guangdong Laboratory (Zhuhai), Zhuhai, 519082, China
[2]Guangdong Provincial Observation and Research Station for Climate Environment and Air Quality Change in the Pearl River Estuary, Key Laboratory of Tropical Atmosphere-Ocean System (Sun Yat-sen University), Ministry of Education, Zhuhai, 519082, China
[3]State Key Joint Laboratory of Environmental Simulation and Pollution Control, The State Environmental Protection Key Laboratory of Atmospheric Ozone Pollution Control, College of Environmental Sciences and Engineering, Peking University, Beijing, 100871, China.
[4]Department of Civil and Environmental Engineering, The Hong Kong Polytechnic University, Hong Kong, 999077, China
[5]Jiangsu Key Laboratory of Atmospheric Environment Monitoring and Pollution Control, Collaborative Innovation Center of Atmospheric Environment and Equipment Technology, Nanjing University of Information Science and Technology, Nanjing, 210044, China

*Correspondence to:* Haichao Wang (wanghch27@mail.sysu.edu.cn), Keding Lu (k.lu@pku.edu.cn)

**ABSTRACT.** Nitrate radical ($NO_3$) is an important nocturnal atmospheric oxidant in the troposphere, which significantly affects the lifetime of pollutants emitted by anthropogenic and biogenic activities, especially volatile organic compounds (VOC). Here, we used one-year VOC observation data obtained in urban Beijing in 2019 to look into the level, compositions, and seasonal variation of $NO_3$ reactivity *(*$k_{NO3}$). We show that hourly $k_{NO3}$ towards measured VOC highly varied from $<10^{-4}$ to 0.083 $s^{-1}$ with a campaign-averaged value (± standard deviation) of 0.0032 ± 0.0042 $s^{-1}$. There was large seasonal difference in $NO_3$ reactivity towards VOC with the average of 0.0024 ± 0.0026 $s^{-1}$, 0.0067 ± 0.0066 $s^{-1}$, 0.0042 ± 0.0037 $s^{-1}$, 0.0027 ± 0.0028 $s^{-1}$ from spring to winter. Alkenes such as isoprene and styrene accounted for the majority. Isoprene was the dominant species in spring, summer, and autumn, accounting for 40.0%, 77.2%, and 43.2%, respectively. Styrene only played a leading role in winter, with a percentage of 39.8%. A sensitivity study shows monoterpenes, the species we did not measure, may account for a large fraction of $k_{NO3}$. Based on the correlation between the calculated $k_{NO3}$ and VOC concentrations in 2019, we established localized parameterization schemes for predicting the reactivity by only using a part of VOC species. The historically published VOC data was collected using the parameterization method to reconstruct the long-term $k_{NO3}$ in Beijing. The lower $k_{NO3}$ during 2014-2021 compared with that during 2005-2013 may attribute to anthropogenic VOC emission reduction. At last, we revealed that $NO_3$ dominated the nocturnal VOC oxidation with 83% on the annual average in Beijing in 2019, which varied

seasonally and was strongly regulated by the level of $k_{NO3}$, nitrogen oxide, and ozone. Our results improve the understanding of nocturnal atmospheric oxidation in urban regions and gain knowledge of nocturnal VOC oxidation and secondary organic pollution.

## 1. Introduction

A large amount of NO emitted in cities is oxidized into $NO_2$ by $O_3$ in the atmosphere (R1), and $NO_2$ continues to be oxidized into nitrate radical ($NO_3$) by $O_3$ (R2). $NO_3$ is the main nocturnal tropospheric oxidant (Brown and Stutz, 2012; Wayne et al., 1991) with a relatively high concentration level at night due to it has rapid loss by photolysis (R3) and the reaction with NO during the daytime (Stark et al., 2007). These two reactions return $NO_3$ back to $NO_x$ and thus cannot contribute to effective $NO_x$ removal. In addition, $NO_3$ reacts with $NO_2$ to form nitrous pentoxide ($N_2O_5$) (R5), and $N_2O_5$ can be decomposed to $NO_3$ and $NO_2$ (R6), establishing a temperature-dependent equilibrium.

$$NO+O_3 \rightarrow NO_2+O_2 \quad (R1)$$

$$NO_2+O_3 \rightarrow NO_3+O_2 \quad (R2)$$

$$NO_3+hv \rightarrow NO+O_2 \quad (R3)$$

$$NO_3+hv \rightarrow NO_2+O^1D \quad (R4)$$

$$NO_3+NO \rightarrow 2NO_2 \quad (R5)$$

$$NO_2+NO_3+M \rightarrow N_2O_5+M \quad (R6)$$

$$N_2O_5+M \rightarrow NO_2+NO_3+M \quad (R7)$$

During the nighttime, there are two kinds of reactions that have a large impact on air pollution and regulate the lifetime and budget of many trace gas species. One is $NO_3$ oxidizes volatile organic compounds and forms complex products (R8). The other is $NO_3$ be transformed into $N_2O_5$ and removed by heterogeneous hydrolysis (R9), providing an effective way to remove $NO_x$ and produce nitrate aerosol and nitryl chloride (Brown et al., 2004; Dentener and Crutz, 1993; Osthoff et al., 2008). The competition between R8 and R9 determines the fate of nocturnal nitrogen oxidation chemistry, which leads to the formation of different secondary pollutants (Bertram and Thornton, 2009; Brown et al., 2006). In particular, the degradation of VOC by $NO_3$, especially biogenic VOC (Ng et al., 2017), has been proven to be related to the formation of organic nitrate and secondary organic aerosols (SOA) (Goldstein and Galbally, 2009; Kiendler-Scharr et al., 2016).

$$NO_3+VOC \rightarrow products \quad (R8)$$

$$N_2O_5+H_2O_{(aq)}/Cl^- \rightarrow HNO_3 + \varphi ClNO_2 \quad (R9)$$

The high $NO_3$ concentration and fast reaction rate make $NO_3$ responsible for the sinking of many unsaturated hydrocarbons at night (Edwards et al., 2017; Ng et al., 2017; Yang et al., 2020). The $NO_3$ reactivity ($k_{NO3}$) towards VOC, defined as the consuming capacity of $NO_3$ by ambient VOC, can be calculated by Eq. 1.

$$k_{NO3} = \sum k_i \times [VOC_i] \qquad \text{Eq. 1}$$

where the $[VOC_i]$ is VOC concentrations and $k_i$ is the corresponding reaction rate coefficients. Table S1 gives the reaction rate coefficients of $NO_3$ with VOC (Atkinson and Arey, 2003). The contribution of VOC to the $NO_3$ reactivity with respect to different VOC varies greatly, which is caused by the abundance of species and the reaction rate coefficients. Thus, $NO_3$ reactivity towards VOC is also affected by temperature since temperature affects not only the temperature-dependent reaction rate coefficients but also the VOC emissions in the atmosphere, especially for the emission of biogenic VOC like isoprene and monoterpenes (Wu et al., 2020), leading to the variations of VOC species that dominate $k_{NO3}$ towards VOC in different seasons.

Previous works showed that the VOC species which dominate the $NO_3$ reactivity vary greatly between different regions. In forests and rural areas, such as Pabstchum outside Berlin, Germany, the lush forests emitted a large number of monoterpenes and isoprene, accounting for the majority of $k_{NO3}$, which ranged from 0.0025 to 0.01 $s^{-1}$ (Asaf et al., 2009). In semi-arid urban areas such as Jerusalem, the emissions of BVOC are less due to the sparser vegetation, and the maximum of $NO_3$ reactivity was about 0.01 $s^{-1}$, in which the phenol, cresol and some monoolefins emitted by road traffic were the main contributors (Asaf et al., 2009). In urban regions like Houston, industrial emissions, including isoprene and other alkenes, dominated the $NO_3$ reactivity (Stutz et al., 2010). In the city's suburbs, the $k_{NO3}$ may be jointly affected by anthropogenic and biogenic volatile organic compounds. For example, the $NO_3$ reactivity towards VOC in Xianghe, Beijing reached 0.024 ± 0.030 $s^{-1}$, with a maximum value of 0.3 $s^{-1}$ and minimum value of 0.0011 $s^{-1}$. Isoprene, styrene, and 2-butene contributed to most of the $k_{NO3}$ (Yang et al., 2020).

The above $NO_3$ reactivities are all calculated by the measurement of VOC concentrations. In addition to this method, an instrument was developed to measure $k_{NO3}$ in the atmosphere directly (Liebmann et al., 2017). They presented the first direct measurement of $NO_3$ reactivity in the Finnish boreal forest in 2017. They concluded that the $NO_3$ reactivity was generally high, with a maximum value of 0.94 $s^{-1}$, displaying a strong diel variation with a nighttime mean value of 0.11 $s^{-1}$ and daytime value of 0.04 $s^{-1}$ (Liebmann et al., 2018a). In 2018, they presented the direct measurement in and above the boundary layer of a mountain site, with daytime values of up to 0.3 $s^{-1}$ and nighttime values close to 0.005 $s^{-1}$ (Liebmann et al., 2018b). Most importantly, the direct measurement revealed the existence of missing $NO_3$ reactivity in various regions, which indicated the missing $NO_3$ oxidation mechanisms. These results largely improved the understanding of nighttime chemistry.

Nevertheless, the direct field determination of $k_{NO3}$ is still extremely lacking, especially in urban regions at the current stage. Until now, most works about the VOC oxidation by $NO_3$ were usually based on short-term investigations, and the analysis of the nocturnal chemical process or reactivity was carried out based on the data of a few weeks or several months. Studies of nighttime chemistry based on long-term measurement data are very scarce (Vrekoussis et al., 2007; Wang et al., 2023;

Zhu et al., 2022). The detailed VOC contributions to $k_{NO3}$, and the relationship between certain VOC and total $NO_3$ reactivity on a long-time scale are also rarely studied. Our recent work reported that the increasing trend of the $NO_3$ production rate is caused by anthropogenic emission changes, while the long-term and detailed $NO_3$ loss budget is still uncertain to some extent (Wang et al., 2023). Here, we attempt to look for insight into the level, variations, and impacts of $NO_3$ reactivity by using the one-year measurement of VOC in an urban site in Beijing, the role of unmeasured VOC species (monoterpenes) in the contributions of $NO_3$ reactivity is also discussed. The long-term trend of $NO_3$ reactivity is estimated by collecting the published VOC data and the newly proposed parameterization method. At last, the nocturnal VOC oxidation by $NO_3$ during different seasons was further evaluated.

## 2. Method

### 2.1 Site description and instrumentation

The measurement was conducted at the campus of Peking University (39° 99' N, 116° 30' E) during the whole year of 2019. The site is situated northeast of the Beijing city center and near two traffic roads, which represent a typical urban and polluted area with fresh, anthropogenic emissions (Wang et al., 2017a). The measurements were made on a building roof with a height of 20 m above the ground. Measurements of VOC concentrations were performed using an automated gas chromatograph equipped with mass spectrometry or flame ionization detectors (GC-MS/FID). The volatile organic compounds were pretreated by pre-freezing and collected in the deactivated quartz empty capillary at extreme-low temperature (-150 ℃), then heated and delivered into the analysis system. After separation by the double chromatographic column, the low-carbon compounds $C_2$-$C_4$ were detected by the FID detector, and the high-carbon compounds $C_5$-$C_{10}$ were detected by the MS detector. There are 56 kinds of VOC measured in total (listed in Table S1 and the concentrations are depicted in Figure S1), in which monoterpenes measurement are not valid. NOx and $O_3$ were monitored by chemiluminescence (Thermo Scientific, 42i-TLE) and UV photometric methods (Thermo Scientific, 49i), respectively. A Tapered Element Oscillating Microbalance analyzer (TianHong, TH-2000Z1) was used to measure the mass concentration of $PM_{2.5}$. The quality assurance and quality controls of data were implemented regularly (Chen et al., 2020). Photolysis frequencies were obtained by the Tropospheric Ultraviolet and Visible (TUV) model simulation. Hourly data were processed and used in the following analysis.

### 2.2 Estimation of monoterpenes

Since the measurement data did not include monoterpenes (MNTs), we, therefore, use the measured isoprene and modeled concentration ratio of monoterpene to isoprene in the same region of the measurement site (named as Factor, Eq. 2) to estimate the ambient monoterpene concentrations (named as $MNT_{obs}$, Eq. 3). The Factor was obtained by the regional model (WRF/CMAQ), more details of the model simulation setup can be found in Mao et al. (2022). Briefly, the regional model CMAQ (Community Multiscale Air Quality) version 5.2 was applied to simulate air quality in

eastern China, with a horizontal resolution of 36 km. Specifically, the gas-phase mechanism of SAPRC-07 and aerosol module AERO6 were used. The meteorological fields were provided by Weather Research & Forecasting (WRF) Model version 4.2. The biogenic emissions were simulated by the MEGANv2.1, which was driven by WRF as well, and the emissions of open burning were estimated with FINN. The MEIC emission inventory for 2019 (obtained via private communication) was used to represent anthropogenic emissions over China, while the emissions in the areas outside China were provided by the REAS v3.2 inventory simulation.

$$Factor = \frac{[MNT_{sim}]}{[ISO_{sim}]} \qquad \text{Eq. 2}$$

$$[MNT_{obs}] = [ISO_{obs}] \times Factor \qquad \text{Eq. 3}$$

We used the Factor to estimate monoterpenes level rather than modeled monoterpene concentrations due to the modeled isoprene is systematically higher than that of observation (Fig. S2). Thus the using of the modeled Factor may be more reasonable. In Beijing, α-pinene and β-pinene were reported to have the highest abundance among monoterpenes (Cheng et al., 2018), with higher emissions in summer (Wang et al., 2018b; Xia and Xiao, 2019). Therefore, we use a weighted reaction rate coefficient approximated by the average value of α-pinene and β-pinene with $NO_3$ in the following calculations. Since the emissions of sesquiterpenes in BVOC are much lower than that of isoprene, monoterpenes, and other BVOC, thus we did not consider the contribution of sesquiterpenes to the reactivity. The detailed average diurnal variations of Factor are listed in Table S2.

## 2.3 VOC oxidation rate by $NO_3$

To study the reaction of $NO_3$ and VOC during the nighttime, we estimated the $NO_3$ concentrations by steady-state calculation. This method is widely used to estimate the concentrations of short-lived substances, by assuming its production and loss rates are balanced in a specific time range. Given sufficient time, the steady state can be reached for $NO_3$ at night, in which the production and loss terms are approximately balanced (Brown, 2003; Crowley et al., 2010). Here the production terms of $NO_3$ are the reaction of $NO_2$ and $O_3$, and the loss terms of $NO_3$ include reactions with VOC, reaction with NO, heterogeneous reaction, and photolysis. The steady-state $NO_3$ mixing ratios are expressed by Eq. 4 (Brown and Stutz, 2012).

$$[NO_3]_{ss} = \frac{k_{NO_2+O_3}[NO_2][O_3]}{\sum k_i \times [VOC_i] + k_{NO+NO_3}[NO] + J_{NO_3} + k_{het}K_{eq}[NO_2]} \qquad \text{Eq. 4}$$

Where $J_{NO3}$ is the sum of the photolysis coefficients of the two photolysis reactions of $NO_3$. The $k_{het}$ is the heterogeneous uptake rate of $N_2O_5$ on the aerosol surface, which can be calculated by Eq. 5.

$$k_{het} = 0.25 \times \gamma \times S_a \times c \qquad \text{Eq. 5}$$

Where $\gamma$ is the dimensionless uptake coefficient of $N_2O_5$ parameterized by Eq. 6 (Evans and Jacob, 2005; Hallquist et al., 2003; Kane et al., 2001), Sa ($m^2\ m^{-3}$) is the aerosol surface area density estimated by the level of $PM_{2.5}$ (Wang et al., 2021), and $c$ is the mean molecular velocity of $N_2O_5$.

$$\gamma = \alpha \times 10^{\beta}$$

$$\alpha = 2.79 \times 10^{-4} + 1.3 \times 10^{-4} \times RH - 3.43 \times 10^{-6} \times RH^2 + 7.52 \times 10^{-8} \times RH^3$$

$$\beta = 4 \times 10^{-2} \times (T - 294) \ \ (T > 282K)$$

$$\beta = -0.48 \ \ (T < 282K) \qquad \text{Eq. 6}$$

The reaction rate coefficients of $NO_2$ and $O_3$, NO and $NO_3$, and the equilibrium constant for the forward and reverse Reactions (R4) and (R5) are temperature dependent. We have adopted JPL evaluation reports for the reaction rate coefficients. The time series of hourly-related parameters in estimating the steady-state $NO_3$ and the diurnal cycle of $NO_3$ concentrations were shown in Fig. S3 and Fig. S4. To compare the VOC oxidation by $NO_3$ with other oxidants, we estimated OH concentrations by the slope extracted from the measured OH and $J_{O1D}$ ($s^{-1}$) in North China (Tan et al., 2017)) (Eq. 7), where $J_{O^1D}$ used in this study was obtained by the TUV model simulations. The VOC oxidation rate ($R_{NO3}$) and the ratio of VOC oxidized by $NO_3$ to the total oxidation rate can be calculated by Eq. 8.

$$[OH] = 4.1 \times 10^{11} cm^{-3} s^{-1} \times J_{O^1D} \qquad \text{Eq. 7}$$

$$R_{NO_3} \approx \frac{\sum k_i \times [VOC_i][NO_3]}{\sum k_i \times [VOC_i][OH] + \sum k_i \times [VOC_i][NO_3] + \sum k_i \times [VOC_i][O_3]} \qquad \text{Eq. 8}$$

where $k_i$ represents the corresponding reaction rate coefficients of different VOC with oxidants.

## 3. Results and discussion

### 3.1 $NO_3$ reactivity calculated by measured VOC

During the campaign, the hourly $k_{NO3}$ towards measured VOC (named as $k_{NO3\_mea}$) highly varied from $<10^{-4}$ to 0.083 $s^{-1}$ with campaign-averaged value (± standard deviation) of 0.0032 ± 0.0042 $s^{-1}$. The $k_{NO3\_mea}$ displayed a strong diel variation on the annual average (Fig. S5). In previous studies, the $NO_3$ reactivity towards VOC was reported to be 0.024 ± 0.030 $s^{-1}$ on average in a suburban site in summer in North China (Yang et al., 2020); and highly varied between 0.005 - 0.3 $s^{-1}$ in the mountaintop site in summer (Liebmann et al., 2018c). Our result is one order of magnitude lower, which may reflect the huge difference of $k_{NO3\_mea}$ in different environments and sampling time. Certainly, it may be attributed to the reason that calculated $k_{NO3}$ here did not include some species, such as monoterpenes, phenol, cresol and so on. The diurnal variations of $k_{NO3\_mea}$ had strong seasonal variability (Fig. S6). The diurnal variations in winter and spring were relatively weak, and in summer and autumn were strong, with clear peaks at 9:00-10:00 and 15:00, respectively. The $k_{NO3\_mea}$ in spring, summer, and autumn reached the daily maximum value between 8:00 a.m. and 10:00 a.m. (spring: 0.0034 $s^{-1}$, summer: 0.0083 $s^{-1}$, autumn: 0.0057 $s^{-1}$). In winter, it reached the maximum value of 0.0033 $s^{-1}$ at about 22:00.

As shown in Fig. 1a, the $k_{NO3\_mea}$ reached the highest in August and lowest in February, which was

largely affected by the level of isoprene and styrene. For example, isoprene contributed ~80% to the reactivity in August. The $k_{NO3\_mea}$ towards isoprene reached the maximum in August and the minimum in February, which was consistent with the previously reported change in isoprene concentrations in Beijing (Cheng et al., 2018). The $k_{NO3\_mea}$ shows a large seasonal difference with the average value of 0.0024 ± 0.0026 $s^{-1}$, 0.0067 ± 0.0066 $s^{-1}$, 0.0042 ± 0.0037 $s^{-1}$, 0.0027 ± 0.0028 $s^{-1}$ from spring to winter. Table S3 shows the specific contributions of the top six species to $k_{NO3\_mea}$ in different seasons. Isoprene was the dominant species, accounting for 40.0%, 77.2%, and 43.2% in spring, summer, and autumn. By comparison, styrene only played a leading role in winter, accounting for 39.8%. Among the species which contributed to $k_{NO3\_mea}$ in Beijing, isoprene and styrene contributed most to the overall $k_{NO3\_mea}$ (60%~90%), followed by cis-2-butene, trans-2-butene, trans-2-pentene, and proplyene (5%~15%) with another VOC less than 2%. Our results are consistent with previous studies in Beijing that $k_{NO3}$ was mainly contributed by isoprene (Yang et al., 2020), indicating the critical role of isoprene in $NO_3$ reactivity in Beijing. From summer to autumn, the dominant species changed from isoprene to styrene, while from winter to spring, the dominant species changed from styrene to isoprene. This indicated the AVOC and BVOC control $k_{NO3\_mea}$ alternately. Overall, the $k_{NO3\_mea}$ displayed a characteristic of high in summer and autumn and low in winter and spring.

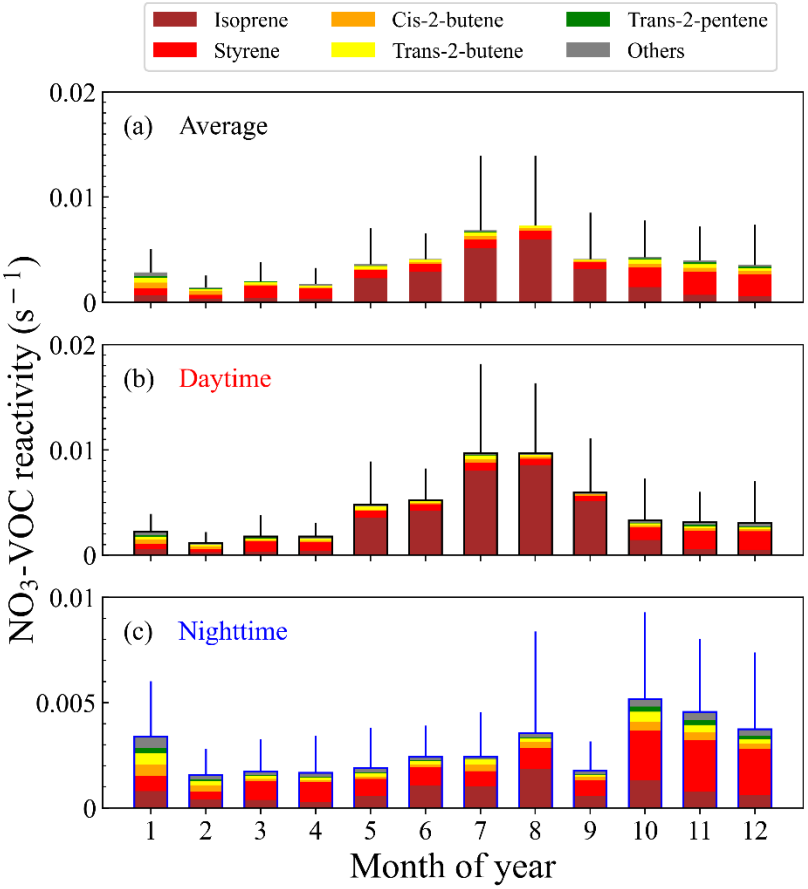


**Figure 1.** Histograms of monthly-averaged $k_{NO3\_mea}$ and the compositions during the day (a), daytime (b), and nighttime (c). The color denotes the contributions of different VOC species. The lines represent the error bars of the reactivity (± standard deviations).

Figure 1b-c shows the $k_{NO3\_mea}$ towards measured VOC display clear day-night differences in summer and winter, especially in summer. The $NO_3$ reactivity towards VOC in the daytime reached the value of 0.010 $s^{-1}$ in July and August, which was much higher than 0.002 $s^{-1}$ in the nighttime. The variations were mainly caused by the diel variations of isoprene concentrations. Reversely, the reactivity was higher at night and lower in the daytime in winter, which was due to the high AVOC level in the morning and at night (Lee and Wang, 2006). Specifically, styrene concentrations at night increased significantly in the stable nocturnal boundary layer, resulting in relatively higher reactivity.

In urban areas of Beijing, isoprene origins from anthropogenic and biogenic sources, which the anthropogenic sources of isoprene are mainly traffic emissions (Li et al., 2013; Riba et al., 1987; Zou et al., 2015). The isoprene emissions from biogenic sources in Beijing were one order of magnitude larger than that of anthropogenic sources (Yuan et al., 2009). This indicates the concentrations of isoprene at the environmental level in the urban areas of Beijing are not affected by the traffic vehicles but mainly by plants (Cheng et al., 2018). As an aromatic hydrocarbon, styrene origins from both anthropogenic and biogenic sources in the atmosphere (Miller et al., 1994; Mogel et al., 2011; Schaeffer et al., 1996; Tang et al., 2000; Zielinska et al., 1996; Zilli et al., 2001), such as the laminar flame of engine fuel (Meng et al., 2016), industrial production (Radica et al., 2021) and other human activities. The dominant source of styrene in Beijing is the local vehicle emissions (Li et al., 2014). Some vegetation, such as evergreen and oleander, can also release natural styrene (Wu et al., 2014), however, due to the dense industrial distribution in the urban area and the much lower level of these biogenic styrene compared with isoprene, we believe that the styrene in the atmosphere in Beijing is mainly resulted from anthropogenic origins. It is believed that human activities in winter, such as heating, gasoline, and diesel combustion, increased, meanwhile, the reduction of temperature and radiation resulted in the reduction of biogenic isoprene emissions, explained the conversion of dominance of $NO_3$ reactivity from summer to winter.

The $NO_3$ reactivity towards MNTs (named as $k_{NO3\_MNTs}$) was estimated by the method mentioned in section 2.2. After taking MNTs into account, the total $k_{NO3}$ (named as $k_{NO3\_total}$) was greatly enlarged, with the campaign-averaged value of 0.0061 ± 0.0088 $s^{-1}$, resulting in our results comparable with previous research results. The $NO_3$ reactivity towards MNTs was higher in autumn and winter and lower in spring and summer (Fig. S7). Considering the corresponding reactivity towards monoterpenes, the total $NO_3$ reactivity towards VOC changed from (summer > autumn > winter > spring) to (autumn > winter > summer > spring), highlighting the impact of the monoterpene variations on the reactivity. The $NO_3$ reactivity towards MNTs displayed significant differences between daytime and nighttime (Fig. S7c-d). The reactivity at night in all months was higher than that in the daytime, especially from October to January, highlighting the role of biogenic monoterpenes in nocturnal $NO_3$ chemistry (Li et al., 2013; Riba et al., 1987). To evaluate the contribution of monoterpenes to the total $k_{NO3}$, we calculated the fraction ($F_{MNTs}$) by Eq. 9.

$$F_{MNTs} = \frac{k_{NO_3\_MNTs}}{k_{NO_3\_total}} \qquad \text{Eq. 9}$$

Figure 2a displays the differences between the $k_{NO3\_mea}$ and $k_{NO3\_total}$. Monoterpenes were very important for $NO_3$ reactivity, and the $F_{MNTs}$ varied from 40% to 80%, with strong seasonal variations. The MNTs accounted for $NO_3$ reactivity of nearly 80% in winter and spring. In the seasons when

isoprene no longer dominated, the measured reactivity accounted for a small fraction, and the corresponding reactivity towards AVOC, such as styrene, was smaller than that of monoterpenes. As shown in Fig. 2b, the measured VOC had high fractions in the daytime and low at night, especially in May and August. The measured VOC in the daytime accounted for more than 60% of $k_{NO3\_total}$, which was closely related to the increasing concentrations of isoprene in the summer daytime. The reactivity towards MNTs accounted for a large fraction of reactivity at night.

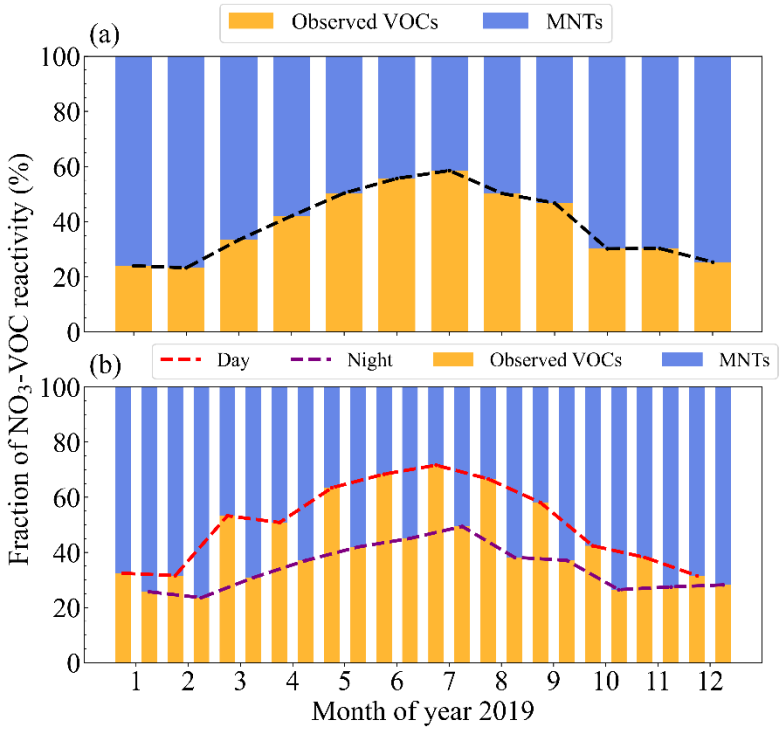


**Figure 2.** (a) Fractions of the $k_{NO3\_total}$. (b) Fractions of the $k_{NO3\_total}$ divided into daytime (left) and nighttime (right). The colors on the stacked bar plot indicate the different fractions as they are donated in the legend. The lines represent the monthly-averaged variations of the $NO_3$ reactivity towards MNTs.

### 3.2 Parameterization of $NO_3$ reactivity

We examined the correlation of key VOC concentrations and $k_{NO3\_mea}$. Figure. S8 gives the case in January, for example. To a certain extent, the variations of $k_{NO3\_mea}$ were closely linked to the variations of the concentrations of main contributors. It is worth noting that in January, trans-2-butene had a higher correlation coefficient with $k_{NO3\_mea}$, which exceeded that of isoprene and styrene. This indicates that higher contributions may not imply a stronger correlation. Fig. 3 shows the correlation coefficients and the fitting equations between VOC concentrations and $k_{NO3}$ in each month (detailed in Table S4). According to the correlation coefficients, we can select the strongest indicator corresponding to a certain month as the variable of the parameterization method. Here we didn't import the VOC with small contributions into the parameterization method because these indicators had no practical significance for $k_{NO3\_mea}$. In this way, we established the first parameterization method (Method 1) by using the strongest indicator in each month which can be found in Table S4 (Eq. 10):

$$NO_3\ reactivity_{sim1} = a \times [VOC] + b \qquad \text{Eq. 10}$$

Where, a, b, and [VOC] respectively represent the slope, the intercept, and the VOC species concentrations (ppbv) used for parameterization each month. The correlation coefficients between isoprene concentrations and $k_{NO3\_mea}$ were high throughout the year, ranging from 0.67 to 0.98, especially in summer. The correlation coefficients between styrene concentrations and the reactivity reached a maximum in autumn and winter, which can display the indication of these two species (isoprene and styrene) in different seasons.

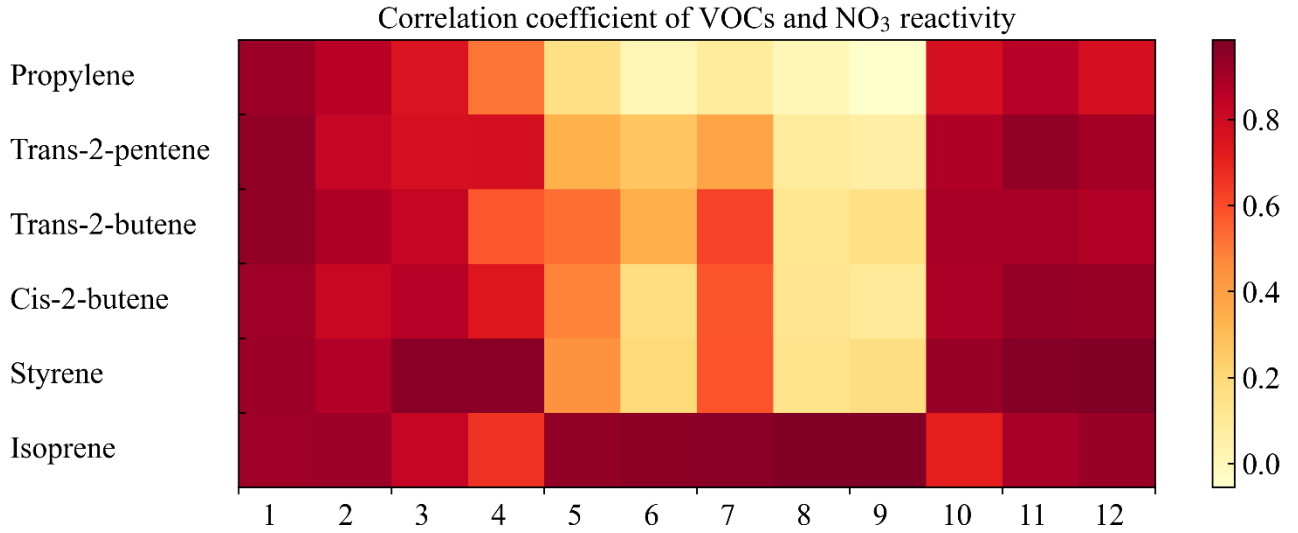


**Figure 3.** The heat map of the monthly correlation between VOC concentrations and $k_{NO3\_mea}$. Colored blocks indicate different correlations by which the best indicator can be selected for the parameterization method of each month.

Besides the indicator parameterization method, we can also select only a part of VOC that contribute most of $k_{NO3\_mea}$ as a representative. Here we approximated $NO_3$ reactivity towards total VOC to the reactivity towards these top 6 species: isoprene, styrene, cis-2-butene, trans-2-butene, trans-2-pentene, and proplyene. Thus, the second parameterization method (Method 2) can be expressed by Eq. 11:

$$NO_3\ reactivity_{sim2} = \sum_{i=1}^{6} k_i \times [VOC_i] \qquad \text{Eq. 11}$$

where $[VOC_i]$ is the VOC concentrations and $k_i$ is the corresponding reaction rate coefficients with $NO_3$. It should be noted that this parameterization method of $NO_3$ reactivity towards VOC may be localized.

To evaluate the effectiveness of the two parameterization methods established above, we estimated the $k_{NO3}$ in the different time scales, and compared them with the determined $k_{NO3\_mea}$ by all measured VOC. As shown in Fig. S9, both methods can well capture the level and variations of $k_{NO3\_mea}$, indicating the parametrization feasibility. Method 1 can easily and quickly estimate $NO_3$ reactivity towards VOC using a single indicator. In areas where a single VOC specie dominates $NO_3$

reactivity towards VOC for a long time, such as forest areas, suburbs, and rural areas (BVOC dominant), this method would have a good performance. Method 2 had a better performance, while more VOC species are needed. In urban areas, especially in urban areas where the contributors had different chemo diversity with strong seasonality, this method should be more suitable. Since the two methods lower the bar for estimating $NO_3$ reactivity by using VOC measurement data, we can investigate the level of $NO_3$ reactivity using the reported VOC measurement data in the past.

We collected the historical measurement data of VOC concentrations in Beijing (Supporting file. S1) and estimated $NO_3$ reactivity using parameterization methods. We found the level of $NO_3$ reactivity mainly ranged from 0.001 to 0.1 $s^{-1}$ in Beijing in the past decades (Fig. 4). During 2014-2020, a large amount of VOC data in urban Beijing presented and be collected in this study. We calculated the $k_{NO3\_mea}$ by detailed VOC concerning the data provided by the literature, and estimated the $NO_3$ reactivity by parameterization methods if the reported data in the literatures are limited. As shown in Fig. 4, $NO_3$ reactivity was relatively lower after 2014 than before. We inferred that the level of isoprene during this period may be varied small since the change of biogenic emission may not be significant. Thus, we proposed that the lower $NO_3$ reactivity during the past decade may be attributed to the anthropogenic emission reduction of anthropogenic VOC. It should be noted that this estimation suffers from uncertainty, nevertheless, this trend and characterization of $NO_3$ reactivity in Beijing is helpful to understand the nighttime chemistry in Beijing.

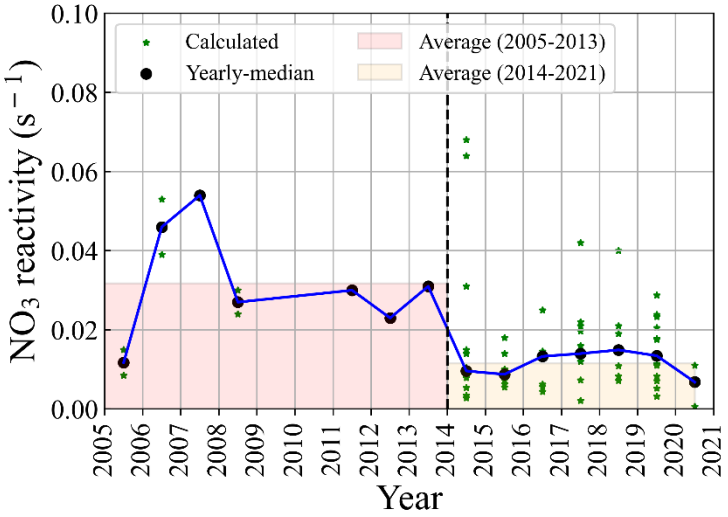


**Figure 4.** The reported VOC concentrations in Beijing calculated the reconstructed $NO_3$ reactivity record from 2005-2021. The averaged $NO_3$ reactivity calculated by the reported VOC data in each campaign is plotted as the star. The median values of $NO_3$ reactivity (black dot) in each year show high during 2005-2013 and relatively low during 2014-2021. It should be noted that the monoterpenes are not considered here.

After considering MNTs, we updated the parameterization method established before by using the relationship between reactivity and VOC concentrations, including monoterpenes. The updated parameterization Method 1 used the same principle introduced in Sect 3.2, with fitting slopes changing significantly (Figure. S10). Table S5 shows the correlation coefficients between six key VOC concentrations and $k_{NO3\_total}$. The updated Method 2 considered the sum contributions of six

VOC and the estimated MNTs by isoprene concentration. We reevaluated the two updated parameterization methods (single VOC and six VOC, respectively). Overall, the performance of the two methods is reasonable, and the updated Method 1 is better than that of Method 2 in general (Fig. S11). We evaluated this parameterization on datasets of other years (shown in Fig S12) and showed a robust performance.

### 3.3 Nighttime VOC oxidation

Here we examined the role of $NO_3$ in VOC oxidation in Beijing 2019. As shown in Fig. S13, OH oxidized most of VOC during the daytime, with the oxidation rate reaching the maximum value of 0.6 pptv $s^{-1}$ in the afternoon. Compared with OH, the VOC oxidation rates by $O_3$ and $NO_3$ in the daytime were remarkably lower. From 18:00 to 6:00, the ratios of VOC oxidized by $NO_3$ kept above 80%, and the contribution of $O_3$ was relatively weak, which is consistent with that reported in high NOx regions(Chen et al., 2019; Edwards et al., 2017; Wang et al., 2018a). The VOC oxidation rate by $NO_3$ presented a single peak at 19:00 with the value of 0.25 pptv $s^{-1}$, which is the same magnitude as that by OH in the daytime, illustrating the importance of $NO_3$ in VOC oxidation as shown in the previous studies (Wang et al., 2017a), implying the importance of nocturnal chemistry for organic nitrate and SOA formation.

The VOC oxidation rate by $NO_3$ and oxidation fractions had strong seasonal variabilities in Beijing. As shown in Fig. 5, the nighttime oxidation rate (summer > spring > autumn > winter) was affected by $NO_3$ concentrations and the total $NO_3$ reactivity towards VOC. In summer, the $NO_3$ oxidation rate presented a single peak, with a maximum value of 0.7 pptv $s^{-1}$ at 20:00, and remained around 0.1 pptv $s^{-1}$ at the rest of the night. The rate at 21:00-5:00 was relatively constant. The rate in winter was lower, with the two maximum values of 0.06 pptv $s^{-1}$ presented at 19:00 and 4:00, which were further lower than the average value of the other three seasons. The results agreed with the previous studies, in which the VOC oxidation rate by $NO_3$ concentrations was high from 19:00-23:00 (Wang et al., 2017b). There was a competition between $NO_3$ and $O_3$ in the nighttime VOC oxidation in Beijing. Although the $NO_3$ oxidation rate at night was higher than that of $O_3$ throughout the year, the changes in $O_3$ oxidation rate significantly impacted the ratios of VOC oxidized by $NO_3$. The ratios of nighttime VOC oxidized by $NO_3$ in Beijing were higher in autumn and spring, summer, and winter. Although the $O_3$ concentrations in winter decreased, the competitiveness of $NO_3$ in VOC oxidation decreased more due to the decline of $NO_3$ concentrations. The competitiveness of $O_3$ in VOC oxidation was relatively enhanced, resulting in a significant decline in the ratios of VOC oxidized by $NO_3$.

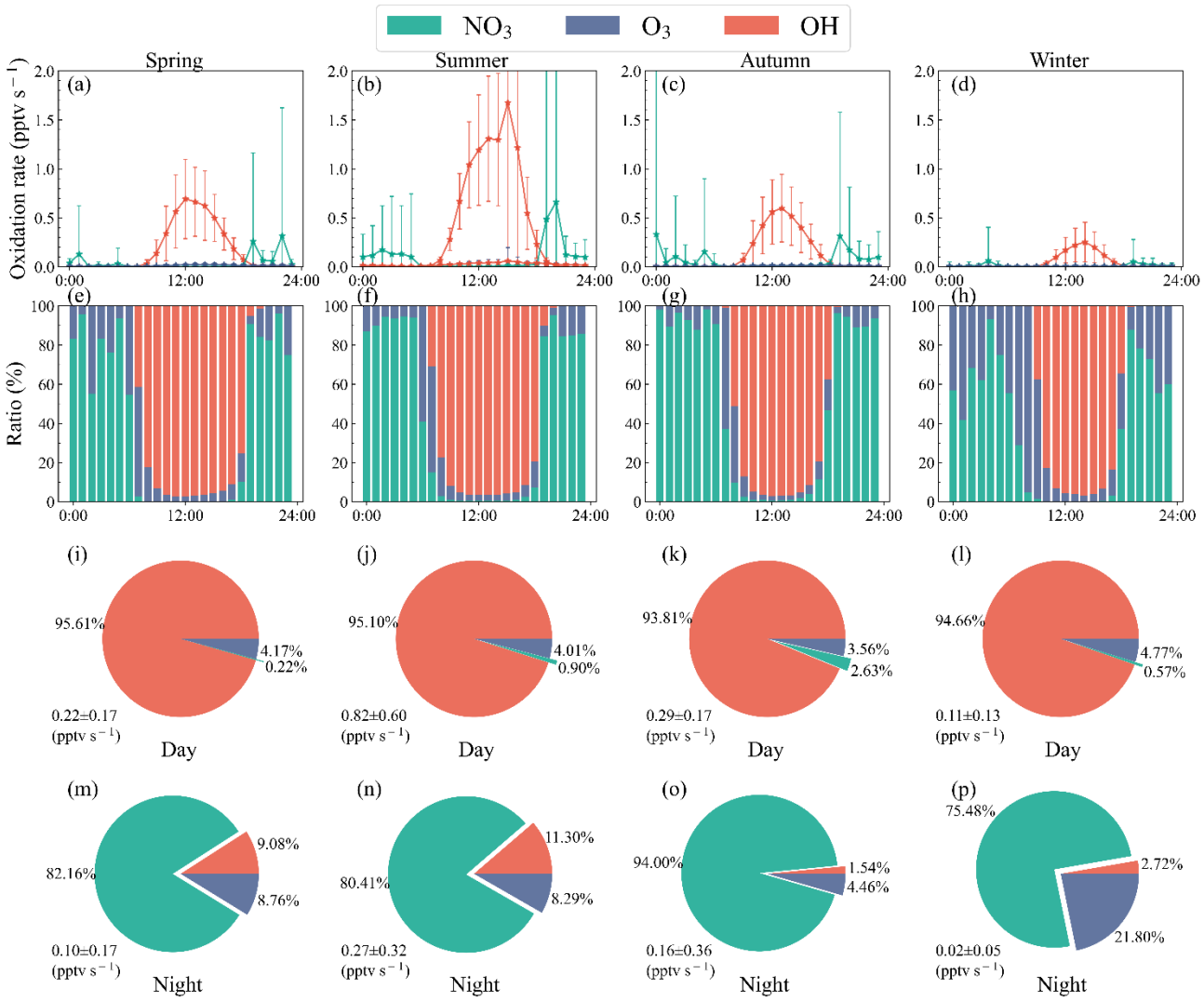


**Figure 5.** (a-d) Median diurnal profiles (±standard deviation) of VOC oxidation rate by atmospheric oxidants in different seasons. (e-h) Fractions of VOC oxidation rate by atmospheric oxidants in different seasons. (i-p) Pie charts representing the daytime and the nighttime VOC oxidation rate by OH, $NO_3$, and $O_3$ during different seasons, with the averaged values and standard deviations.

### 3.4 Relationship between $O_3/NO_x$ and nocturnal VOC oxidation by $NO_3$

To understand the importance of nighttime VOC oxidized by $NO_3$, we defined the fraction of VOC oxidation rate by $NO_3$ to the total oxidation rate as nocturnal VOC oxidation ratio by $NO_3$ ($R_{NO3}$, see Section 2.3 for its calculation) and explored the relationship between the ratio and the nighttime concentrations of $O_3$ and $NO_x$. It is found that a strong nonlinear relationship between them (shown in Figure 6). The $R_{NO3}$ had negative correlation coefficients with NO concentrations. With the increase of NO concentrations at night, the ratios decreased exponentially. When the NO concentrations increased at low NO conditions, it could cause a significant decline in the ratios of VOC oxidized by $NO_3$. While at high NO condition, the ratios were not sensitive to the increase of NO concentrations (Fig. S14), indicating that the nighttime NO concentrations in Beijing strongly controlled the ratios effectively. It can be expected since the increase of NO concentrations controlled the $NO_3$ loss term, then caused the decrease of $NO_3$ concentration. When the NO concentrations

exceeded a threshold value (7 ppbv), the $NO_3$ loss was dominated by NO.

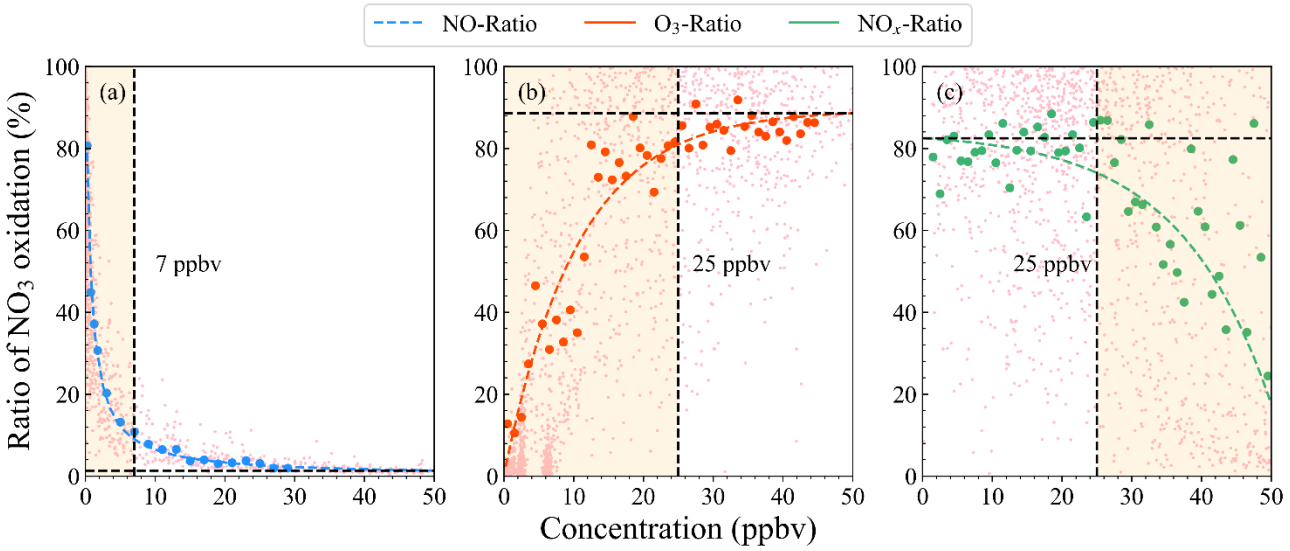


**Figure 6.** Fitting diagrams between the ratios of nighttime VOC oxidized by $NO_3$ and the concentrations of NO (a), $O_3$ (b), and $NO_x$ (c). The light pink scattered dots represent the oxidation ratios at different concentrations, and the solid dots represent the median value of each bin of oxidation ratios corresponding to each concentration range. Colored dot lines represent the fitting results of the solid median dots. And the black dot line in each panel shows a threshold to divide the curve into two regimes. In (a), the regime is divided into NO-limited (<7 ppbv) and NO-saturated (>7 ppbv); in (b) and (c), a threshold of 25 ppbv divide the curves into $NO_x$ ($O_3$) limited and saturated regimes. The results showed in (b) and (c) are representative of low NO condition (< 7 ppbv).

The ratios of nighttime VOC oxidized by $NO_3$ also had a strong nonlinear relationship with $O_3$ and $NO_x$ concentrations. $O_3$ concentrations have one positive and one negative contribution to the $R_{NO3}$. The positive effect is that increasing $O_3$ concentration increases the $NO_3$ production rate, which increases the $NO_3$ steady-state concentrations and then increase the ratios. And the negative is increasing $O_3$ concentrations increases the reaction rate between VOC and $O_3$, which increase the competitiveness of $O_3$ in VOC oxidation and then decrease the ratios. Figure. S14 also shows the relationship between the $R_{NO3}$ and the concentrations of $O_3$. While $O_3$ concentrations were below 25 ppbv, the ratios were very sensitive to $O_3$ level, which fast increased with $O_3$ concentrations. While the ratio became not sensitive and remained relatively constant when the $O_3$ concentrations exceeded 25 ppbv. It can be explained that when the $O_3$ concentrations were low, the $NO_3$ production rate was more sensitive to the increase in $O_3$ concentrations. In this case, $O_3$ mainly affects the ratios positively. When the $O_3$ concentrations were high, the positive effect of $O_3$ tended to be constant, indicating the two opposite effects kept in balance.

When the $NO_x$ concentrations were low (i.e., <25 ppbv), the $R_{NO3}$ was less sensitive to $NO_x$, remaining relatively constant with further increase. The increase of $NO_3$ loss rates through the $N_2O_5$ heterogeneous reaction and the NO reaction was believed to be kept in balance with the $NO_3$ production rate increased by $NO_2$ concentrations. At high $NO_x$ conditions, the ratios sensitively

decreased with the increase of $NO_x$ concentrations, which is explained by the increase of $NO_3$ loss rates by NO, resulting in a decline in the ratios.

To better understand the nonlinear effect of $NO_2$ and $O_3$ on the nighttime VOC oxidation, we further explored the effect of $O_3$ concentration on the ratios existing in different concentrations of $NO_2$. As shown in Fig. S15, in higher concentrations of $NO_2$, the threshold of lower $O_3$ concentrations was required for the $R_{NO3}$ to become constant, which reflected the couple influences of $NO_2$ and $O_3$ on nighttime VOC oxidation through the nonlinear response, and indicated that in the environment richen in $NO_2$, nocturnal $NO_3$ chemistry easily tended to be more dominant.

## 4. Conclusions and implications

In this study, we showed that the $NO_3$ reactivity towards measured VOC highly varied with big seasonal differences, mainly driven by isoprene concentrations. The top 6 contributors to the measured $NO_3$ reactivity towards VOC were isoprene, styrene, cis-2-butene, trans-2-butene, trans-2-pentene, and propylene. Among them, isoprene and styrene contributed most of the reactivity. In addition, monoterpenes are proposed to be a significant source of $NO_3$ reactivity. Recently studies showed that anthropogenic emissions contribute significantly to the ambient MNTs concentrations through biomass burning, traffic and volatile chemical product emissions in the urban regions, it would further enhance the importance of nocturnal $NO_3$ oxidation (Coggon et al., 2021; Nelson et al., 2021; Peng et al., 2022; Qin et al., 2020; Wang et al., 2022). It should be noted that the estimated contributions of MNTs only considered the biogenic emissions and may represent the lower bias. Thus we highlight the importance of field observation of MNTs for advancing the understanding the nighttime $NO_3$ chemistry. In addition, it should be noted that we didn't take the contributions of OVOC into account since the reaction rate coefficients of OVOC with $NO_3$ are small (Ambrose et al., 2007).

Looking for insight to the trend and evolution of detailed $NO_3$ chemistry is very scare, but it can be helpful to understand the response of the nocturnal chemistry on the emission change at a large time scale. Limited by the non-extensive and non-continuous observation, we cannot obtain the long-time measurement of all the VOC species in multiple sites. Since isoprene and styrene are good indicators of $NO_3$ reactivity in different seasons, at least as we showed in urban Beijing, those can be used to estimate the $NO_3$ reactivity towards VOC to reestablish the long-term trend of $NO_3$ reactivity in urban regions for further evaluation of its history of nighttime chemistry. We admitted that the estimation of the $NO_3$ reactivity trend might be highly uncertain, but this attempt may be very helpful to know the level and overall change of nighttime chemistry.

We showed that $NO_3$ dominated the nighttime VOC oxidation in Beijing, but the oxidation ratio had a strong nonlinear relationship with $O_3$ and $NO_x$ concentrations. With the $NO_2$ concentrations decreasing, the threshold values of $O_3$ between the sensitive regime and non-sensitive regime tended to increase, indicative of the nighttime oxidation by $NO_3$ would be more easily affected by the level of $O_3$ with the implementation of sustaining $NO_x$ reduction in the future. The threshold values of $O_3$ can provide an effective basis for the measures to control nocturnal chemical and secondary organic aerosol pollution in the typical urban region.

**Code/Data availability.** The datasets used in this study are available from the corresponding author upon request (wanghch27@mail.sysu.edu.cn; k.lu@pku.edu.cn).

**Author contributions.** H.C.W. and K.D.L. designed the study. H.J.H. and H.C.W. analyzed the data with input from J.W., Z.L.Z., X.Z.X., T.Y.Z., X.R.C., X.L., and S.J.F., W.X.F. provided the modeled monoterpene and isoprene data, X.L., L.M.Z., M.H., and Y.H.Z. organized this field campaign and provided the field measurement dataset. H.J.H. and H.C.W. wrote the paper with input from K.D.L.

**Competing interests**. The authors declare that they have no conflicts of interest.

**Acknowledgments**. This project is supported by the National Natural Science Foundation of China (42175111, 21976006), the Fundamental Research Funds for the Central Universities, Sun Yat-sen University (23lgbj002), the Guangdong Major Project of Basic and Applied Basic Research (grant no. 2020B0301030004). Thanks for the data contributed by the field campaign team.

## Reference.


Ambrose JL, Mao H, Mayne HR, Stutz J, Talbot R, Sive BC. Nighttime nitrate radical chemistry at Appledore island, Maine during the 2004 international consortium for atmospheric research on transport and transformation. Journal of Geophysical Research-Atmospheres 2007; 112: 19.

Asaf D, Pedersen D, Matveev V, Peleg M, Kern C, Zingler J, et al. Long-Term Measurements of NO3 Radical at a Semiarid Urban Site: 1. Extreme Concentration Events and Their Oxidation Capacity. Environmental Science & Technology 2009; 43: 9117-9123.

Atkinson R, Arey J. Atmospheric degradation of volatile organic compounds. Chemical Reviews 2003; 103: 4605-4638.

Bertram TH, Thornton JA. Toward a general parameterization of N2O5 reactivity on aqueous particles: the competing effects of particle liquid water, nitrate and chloride. Atmospheric Chemistry and Physics 2009; 9: 8351-8363.

Brown SS. Applicability of the steady state approximation to the interpretation of atmospheric observations of NO3and N2O5. Journal of Geophysical Research 2003; 108.

Brown SS, Dibb JE, Stark H, Aldener M, Vozella M, Whitlow S, et al. Nighttime removal of NOx in the summer marine boundary layer. Geophysical Research Letters 2004; 31: 5.

Brown SS, Ryerson TB, Wollny AG, Brock CA, Peltier R, Sullivan AP, et al. Variability in nocturnal nitrogen oxide processing and its role in regional air quality. Science 2006; 311: 67-70.

Brown SS, Stutz J. Nighttime radical observations and chemistry. Chemical Society Reviews 2012; 41: 6405-6447.

Chen X, Wang H, Liu Y, Su R, Wang H, Lou S, et al. Spatial characteristics of the nighttime oxidation capacity in the Yangtze River Delta, China. Atmospheric Environment 2019; 208: 150-157.

Cheng X, Li H, Zhang YJ, Li YP, Zhang WQ, Wang XZ, et al. Atmospheric isoprene and monoterpenes in a typical urban area of Beijing: Pollution characterization, chemical reactivity and source identification. Journal of Environmental Sciences 2018; 71: 150-167.

Coggon MM, Gkatzelis GI, McDonald BC, Gilman JB, Schwantes RH, Abuhassan N, et al. Volatile chemical product emissions enhance ozone and modulate urban chemistry. Proceedings of the National Academy of Sciences of the United States of America 2021; 118.

Crowley JN, Schuster G, Pouvesle N, Parchatka U, Fischer H, Bonn B, et al. Nocturnal nitrogen oxides at a rural mountain-site in south-western Germany. Atmospheric Chemistry and Physics 2010; 10: 2795-2812.

Dentener FJ, Crutz PJ. Reaction of N2O5on tropospheric aerosols: impact on the global distributions of NOx, O3, OH. Journal of Geophysical Research 1993; 98: 7149-7163.

Edwards PM, Aikin KC, Dube WP, Fry JL, Gilman JB, de Gouw JA, et al. Transition from high- to low-NOx control of night-time oxidation in the southeastern US. Nature Geoscience 2017; 10: 490-+.

Evans MJ, Jacob DJ. Impact of new laboratory studies of N2O5 hydrolysis on global model budgets of tropospheric nitrogen oxides, ozone, and OH. Geophysical Research Letters 2005; 32: 4.

Goldstein AH, Galbally IE. Known and unexplored organic constituents in the Earth's atmosphere. Geochimica Et Cosmochimica Acta 2009; 73: A449-A449.

Hallquist M, Stewart DJ, Stephenson SK, Cox RA. Hydrolysis of N2O5 on sub-micron sulfate aerosols. Physical Chemistry Chemical Physics 2003; 5: 3453-3463.

Kane SM, Caloz F, Leu MT. Heterogeneous Uptake of Gaseous $N_2O_5$ by $(NH_4)_2SO_4$, $NH_4HSO_4$, and $H_2SO_4$ Aerosols. The Journal of Physical Chemistry A 2001; 105: 6465-6470.

Kiendler-Scharr A, Mensah AA, Friese E, Topping D, Nemitz E, Prevot ASH, et al. Ubiquity of organic nitrates from nighttime chemistry in the European submicron aerosol. Geophysical Research Letters 2016; 43: 7735-7744.

Lee BS, Wang JL. Concentration variation of isoprene and its implications for peak ozone concentration. Atmospheric Environment 2006; 40: 5486-5495.

Li L, Li H, Zhang XM, Wang L, Xu LH, Wang XZ, et al. Pollution characteristics and health risk assessment of benzene

528 homologues in ambient air in the northeastern urban area of Beijing, China. Journal of Environmental Sciences
529 2014; 26: 214-223.
530 Li L, Wu F, Meng X. Seasonal and Diurnal Variation of Isoprene in the Atmosphere of Beijing. Environmental
531 Monitoring in China 2013; 29: 120-124.
532 Liebmann J, Karu E, Sobanski N, Schuladen J, Ehn M, Schallhart S, et al. Direct measurement of NO3 radical reactivity
533 in a boreal forest. Atmospheric Chemistry and Physics 2018a; 18: 3799-3815.
534 Liebmann JM, Muller JBA, Kubistin D, Claude A, Holla R, Plass-Dulmer C, et al. Direct measurements of NO3
535 reactivity in and above the boundary layer of a mountaintop site: identification of reactive trace gases and
536 comparison with OH reactivity. Atmospheric Chemistry and Physics 2018b; 18: 12045-12059.
537 Liebmann JM, Muller JBA, Kubistin D, Claude A, Holla R, Plass-Dülmer C, et al. Direct measurements of
538 NO<sub>3</sub> reactivity in and above the boundary layer of a mountaintop site: identification of
539 reactive trace gases and comparison with OH reactivity. Atmospheric Chemistry and Physics 2018c; 18:
540 12045-12059.
541 Liebmann JM, Schuster G, Schuladen JB, Sobanski N, Lelieveld J, Crowley JN. Measurement of ambient NO3 reactivity:
542 design, characterization and first deployment of a new instrument. Atmospheric Measurement Techniques 2017;
543 10: 1241-1258.
544 Mao J, Li L, Li J, Sulaymon ID, Xiong K, Wang K, et al. Evaluation of Long-Term Modeling Fine Particulate Matter and
545 Ozone in China During 2013–2019. Frontiers in Environmental Science 2022; 10.
546 Meng X, Hu EJ, Li XT, Huang ZH. Experimental and kinetic study on laminar flame speeds of styrene and ethylbenzene.
547 Fuel 2016; 185: 916-924.
548 Miller RR, Newhook R, Poole A. Styrene production, use and human exposure. Critical Reviews in Toxicology 1994; 24:
549 S1-S10.
550 Mogel I, Baumann S, Bohme A, Kohajda T, von Bergen M, Simon JC, et al. The aromatic volatile organic compounds
551 toluene, benzene and styrene induce COX-2 and prostaglandins in human lung epithelial cells via oxidative
552 stress and p38 MAPK activation. Toxicology 2011; 289: 28-37.
553 Nelson BS, Stewart GJ, Drysdale WS, Newland MJ, Vaughan AR, Dunmore RE, et al. In situ ozone production is highly
554 sensitive to volatile organic compounds in Delhi, India. Atmospheric Chemistry and Physics 2021; 21:
555 13609-13630.
556 Ng NL, Brown SS, Archibald AT, Atlas E, Cohen RC, Crowley JN, et al. Nitrate radicals and biogenic volatile organic
557 compounds: oxidation, mechanisms, and organic aerosol. Atmospheric Chemistry and Physics 2017; 17:
558 2103-2162.
559 Osthoff HD, Roberts JM, Ravishankara AR, Williams EJ, Lerner BM, Sommariva R, et al. High levels of nitryl chloride
560 in the polluted subtropical marine boundary layer. Nature Geoscience 2008; 1: 324-328.
561 Peng Y, Mouat AP, Hu Y, Li M, McDonald BC, Kaiser J. Source appointment of volatile organic compounds and
562 evaluation of anthropogenic monoterpene emission estimates in Atlanta, Georgia. Atmospheric Environment
563 2022; 288.
564 Qin M, Murphy BN, Isaacs KK, McDonald BC, Lu Q, McKeen SA, et al. Criteria pollutant impacts of volatile chemical
565 products informed by near-field modelling. Nature Sustainability 2020; 4: 129-137.
566 Radica F, Della Ventura G, Malfatti L, Guidi MC, D'Arco A, Grilli A, et al. Real-time quantitative detection of styrene in
567 atmosphere in presence of other volatile-organic compounds using a portable device. Talanta 2021; 233: 7.
568 Riba ML, Tathy JP, Tsiropoulos N, Monsarrat B, Torres L. Diurnal variation in the concentration of α- and β-pinene in
569 the landes forest (France). Atmospheric Environment 1987; 21: 191-193.
570 Schaeffer V, Bhooshan B, Chen S, Sonenthal J, Hodgson A. Characterization of Volatile Organic Chemical Emissions
571 From Carpet Cushions. Journal of the Air & Waste Management Association (1995) 1996; 46: 813-820.

Stark H, Lerner BM, Schmitt R, Jakoubek R, Williams EJ, Ryerson TB, et al. Atmospheric in situ measurement of nitrate radical (NO3) and other photolysis rates using spectroradiometry and filter radiometry. Journal of Geophysical Research-Atmospheres 2007; 112: 11.

Stutz J, Wong KW, Lawrence L, Ziemba L, Flynn JH, Rappengluck B, et al. Nocturnal NO3 radical chemistry in Houston, TX. Atmospheric Environment 2010; 44: 4099-4106.

Tan ZF, Fuchs H, Lu KD, Hofzumahaus A, Bohn B, Broch S, et al. Radical chemistry at a rural site (Wangdu) in the North China Plain: observation and model calculations of OH, HO2 and RO2 radicals. Atmospheric Chemistry and Physics 2017; 17: 663-690.

Tang WC, Hemm I, Eisenbrand G. Estimation of human exposure to styrene and ethylbenzene. Toxicology 2000; 144: 39-50.

Vrekoussis M, Mihalopoulos N, Gerasopoulos E, Kanakidou M, Crutzen PJ, Lelieveld J. Two-years of NO3 radical observations in the boundary layer over the Eastern Mediterranean. Atmospheric Chemistry and Physics 2007; 7: 315-327.

Wang H, Lu K, Chen X, Zhu Q, Chen Q, Guo S, et al. High N2O5 Concentrations Observed in Urban Beijing: Implications of a Large Nitrate Formation Pathway. Environmental Science & Technology Letters 2017a; 4: 416-420.

Wang H, Lu K, Guo S, Wu Z, Shang D, Tan Z, et al. Efficient N2O5 uptake and NO3 oxidation in the outflow of urban Beijing. Atmospheric Chemistry and Physics 2018a; 18: 9705-9721.

Wang H, Ma X, Tan Z, Wang H, Chen X, Chen S, et al. Anthropogenic monoterpenes aggravating ozone pollution. National Science Review 2022.

Wang H, Wang H, Lu X, Lu K, Zhang L, Tham YJ, et al. Increased night-time oxidation over China despite widespread decrease across the globe. Nature Geoscience 2023.

Wang HC, Lu KD, Chen SY, Li X, Zeng LM, Hu M, et al. Characterizing nitrate radical budget trends in Beijing during 2013-2019. Science of the Total Environment 2021; 795: 9.

Wang HC, Lu KD, Guo S, Wu ZJ, Shang DJ, Tan ZF, et al. Efficient N2O5 uptake and NO3 oxidation in the outflow of urban Beijing. Atmospheric Chemistry and Physics 2018b; 18: 9705-9721.

Wang HC, Lu KD, Tan ZF, Sun K, Li X, Hu M, et al. Model simulation of NO3, N2O5 and ClNO2 at a rural site in Beijing during CAREBeijing-2006. Atmospheric Research 2017b; 196: 97-107.

Wayne RP, Barnes I, Biggs P, Burrows JP, Canosa-Mas CE, Hjorth J, et al. The nitrate radical: physics, chemistry, and the atmosphere. Atmospheric Environment, Part A (General Topics) 1991; 25A: 1-203.

Wu K, Yang X, Chen D, Gu S, Lu Y, Jiang Q, et al. Estimation of biogenic VOC emissions and their corresponding impact on ozone and secondary organic aerosol formation in China. Atmospheric Research 2020; 231.

Wu L, Sun Y, Tian Y, Su D. Composition Spectrum of Biogenic Volatile Organic Compounds Released by Typical Flowers in Beijing. Enuivonmental Science and Technology 2014; 37: 154-158.

Xia C, Xiao L. Estimation of biogenic volatile organic compounds emissions in Jing-Jin-Ji. Acta Scientiae Circumstantiae 2019; 39: 2680-2689.

Yang Y, Wang YH, Zhou PT, Yao D, Ji DS, Sun J, et al. Atmospheric reactivity and oxidation capacity during summer at a suburban site between Beijing and Tianjin. Atmospheric Chemistry and Physics 2020; 20: 8181-8200.

Yuan ZB, Lau AKH, Shao M, Louie PKK, Liu SC, Zhu T. Source analysis of volatile organic compounds by positive matrix factorization in urban and rural environments in Beijing. Journal of Geophysical Research-Atmospheres 2009; 114: 14.

Zhu J, Wang S, Zhang S, Xue R, Gu C, Zhou B. Changes in NO3 Radical and Its Nocturnal Chemistry in Shanghai From 2014 to 2021 Revealed by Long-Term Observation and a Stacking Model: Impact of China's Clean Air Action Plan. Journal of Geophysical Research: Atmospheres 2022; 127.

616 Zielinska B, Sagebiel JC, Harshfield G, Gertler AW, Pierson WR. Volatile organic compounds up to C-20 emitted from
617 motor vehicles; Measurement methods. Atmospheric Environment 1996; 30: 2269-2286.
618 Zilli M, Palazzi E, Sene L, Converti A, Del Borghi M. Toluene and styrene removal from air in biofilters. Process
619 Biochemistry 2001; 37: 423-429.
620 Zou Y, Deng X, Li F, Wang B, Tan H, Deng T, et al. Variation characteristics,chemical reactivity and sources of isoprene
621 in the atmosphere of Guangzhou. Acta Scientiae Circumstantiae 2015; 35: 647-655.
622